

Rietveld refinement on XRD and TEM study of nanocrystalline $\text{PbZr}_{0.5}\text{Ti}_{0.5}\text{O}_3$ ceramics prepared with a soft chemistry route

T.K. MANDAL*

Faculty of Science and Technology, The ICFAI University, Rajawala Road, Central Hope Town, Selaqui, Dehradun-248197, Uttarakhand, India

$\text{PbZr}_{0.5}\text{Ti}_{0.5}\text{O}_3$ nanopowders (~ 27 nm) have been prepared by a controlled reconstructive thermal decomposition and crystallization from an amorphous polymeric precursor with polyvinyl alcohol (PVA) and sucrose at 400 to 700 °C in air. The Rietveld refinement of the XRD profiles which were recorded at room temperature for the $\text{PbZr}_{0.5}\text{Ti}_{0.5}\text{O}_3$ powder prepared by a thermal treatment at 700 °C for 2 h, confirmed the P4mm tetragonal crystal structure of the as prepared $\text{PbZr}_{0.5}\text{Ti}_{0.5}\text{O}_3$ nanopowders, with $a = 0.4036$ nm and $c = 0.4147$ nm. A hexagonal symmetry (R3c), with $a = 0.5774$ nm and $c = 1.4212$ nm, was also detected from Rietveld refinement analysis. Thus, tetragonal and hexagonal phases were found to coexist with the as prepared $\text{PbZr}_{0.5}\text{Ti}_{0.5}\text{O}_3$ nanopowders. The average particle size (D) of the $\text{PbZr}_{0.5}\text{Ti}_{0.5}\text{O}_3$ powders, estimated with the help of the specific surface area, measured by BET method, was 26.1 nm. Average D value, calculated by $\Delta 2\theta_{1/2}$ in the XRD peaks with the Debye-Scherrer relation was ~ 24 nm. TEM study made it possible to measure the particle size of $\text{PbZr}_{0.5}\text{Ti}_{0.5}\text{O}_3$ powders with an average diameter of 27 nm.

Keywords: precursor method; $\text{PbZr}_{0.5}\text{Ti}_{0.5}\text{O}_3$ nanopowders; tetragonal phase; PVA-sucrose; ferroelectrics

© Wrocław University of Technology.

1. Introduction

Lead zirconate titanate (PZT) ceramics have important technological applications in nonvolatile memories, actuators, ultrasonic sensors, infrared detectors and electrooptic devices [1–12]. PZT solid solutions have attracted special attention since they exhibit an unusual phase boundary, which divides regions with rhombohedral and tetragonal structures, called the morphotropic phase boundary (MPB) by Jaffe et al. [1]. The MPB separates a rhombohedral Zr-rich phase from a tetragonal Ti-rich phase. The dielectric constant, piezoelectric constant and electromechanical coupling coefficients all show a pronounced maximum values for the composition corresponding to the MPB [1, 13]. The ferroelectric region of the phase diagram consists mainly of two different regions: the Zr-rich rhombohedral region that

contains two phases with space groups R3m and R3c, and the Ti-rich tetragonal region, with a space group P4mm [14]. According to the phase boundary model of Jaffe et al., the MPB in $\text{PbZr}_x\text{Ti}_{1-x}\text{O}_3$ ($0 \leq x \leq 1$) lies at $x \sim 0.5$ [1]. A number of workers have reported their interesting results about the MPB and this region is frequently reported as the region of phase coexistence whose width depends on the method of sample preparations as well as sample processing conditions [5, 13–15].

In order to achieve the super performance of devices with small physical volume, the present trend is to make devices with smaller and smaller sizes, which requires fine-grained ceramics with uniform microstructures. Therefore, recently, there has been a serious competition in developing processing methods, which would produce PZT powders with a fine particle size and high chemical homogeneity, since both the features are important to obtain ceramics with a controlled

*E-mail: tapanm@yahoo.com

microstructure [5]. Microstructure, i.e. grain size, morphology of grains and their distribution and composition of PZT ceramics play a vital role in determining polarization, coercivity and T_C values.

Traditionally, PZT ceramics are prepared by solid-state reaction processes from their oxide mixtures [16]. The conventional methods involve a calcination process at a high temperature ($>1200\text{ }^\circ\text{C}$) to synthesize PZT perovskite powders [17]. Several surface analysis techniques in pure and doped materials [18] have confirmed the presence of chemical inhomogeneities and compositional fluctuations in PZT ceramics prepared from oxide mixtures [19]. Surowiak et al. [20] exploited sol-gel process to obtain fine-grained (average dimension of the grains of 0.3 to 3 μm and mean dimension of the crystallites, $\bar{D} \approx 30\text{ nm}$) amorphous nanopowders of the solid solution $\text{PbZr}_{0.5}\text{Ti}_{0.5}\text{O}_3$, at a temperature of 927 $^\circ\text{C}$. Zeng et al. [21] explored sol-gel process for the synthesis of $\text{PbZr}_{0.5}\text{Ti}_{0.5}\text{O}_3$ thin films. Sol-gel method was also used by Wu et al. [22] for the synthesis of submicrometer-sized $\text{PbZr}_{0.52}\text{Ti}_{0.48}\text{O}_3$ powders. However, the metal alkoxides used in sol-gel method, for the preparation of PZT, are generally expensive and are well known for their high sensitivity to moisture [21]. In addition, these metal-alkoxides are very unstable, because of the high electropositive nature of the metal atoms [22]. Some workers reported that a controlled atmosphere (dry argon or nitrogen gas) must be used to the synthesis of PZT through sol-gel method [22, 23].

In the present investigation, the author explores a chemical method [5] with a reactive polymer matrix of polyvinyl alcohol (PVA) and sucrose polymer molecules and applies it to synthesize $\text{PbZr}_{0.5}\text{Ti}_{0.5}\text{O}_3$ nanoparticles. The present method involves a reconstructive molecular decomposition of the polymeric precursor followed by a self-controlled recrystallization of the ceramic nanoparticles at 400 to 700 $^\circ\text{C}$. The as prepared nanoparticles of $\text{PbZr}_{0.5}\text{Ti}_{0.5}\text{O}_3$ exhibit the coexistence of tetragonal and hexagonal phases. The structure of the formed nanoparticles has been analyzed with X-ray diffraction and TEM. Rietveld refinement analysis of X-ray diffraction has been

utilized to characterize the structure of the prepared $\text{PbZr}_{0.5}\text{Ti}_{0.5}\text{O}_3$ nanopowders.

2. Experimental

The synthesis of $\text{PbZr}_{0.5}\text{Ti}_{0.5}\text{O}_3$ precursor solution was carried out from the starting materials (99.99 % pure) of $\text{Pb}(\text{NO}_3)_2$, $\text{ZrOCl}_2 \cdot 8\text{H}_2\text{O}$ and TiO_2 in the stoichiometric ratio of 1:0.5:0.5. At first, $\text{ZrOCl}_2 \cdot 8\text{H}_2\text{O}$ (dissolved in deionized water) and TiO_2 (dissolved in 48 % HF) were precipitated as hydrated hydroxides by hydrolysis with NH_4OH in cold water at 2 to 5 $^\circ\text{C}$ (with stirring). The precipitates were repeatedly washed with deionized water to remove chloride ions and other byproduct impurities. Then, they were dissolved in HNO_3 and mixed together with an aqueous $\text{Pb}(\text{NO}_3)_2$ solution in requisite amounts. The obtained precursor solution was added dropwise to an aqueous polymer solution of PVA and sucrose at room temperature with stirring. It resulted in a stable transparent solution with Pb^{2+} , Zr^{4+} and Ti^{4+} metal cations rearranged in a specific structure through the polymer molecules. An amorphous structure of the polymer precursor solution was retained (as confirmed by the X-ray diffraction) after drying it at room temperature or even at higher temperatures in the 60 to 80 $^\circ\text{C}$ ranges. The product was pulverized by grinding in a mortar with a pestle by hand. It consisted of a voluminous porous mass in a characteristic black color of refined polymer molecules encapsulating the metal cations. This carbonaceous mass decomposed at 350 to 450 $^\circ\text{C}$ in air, leaving behind a recrystallized $\text{PbZr}_{0.5}\text{Ti}_{0.5}\text{O}_3$ nanopowder. Several batches of the specimen were, thus, derived by heating the polymer precursor in air at 400 to 700 $^\circ\text{C}$ for 2 h.

X-ray diffraction of the specimens was recorded with PW 1710 X-ray diffractometer using 0.15418 nm $\text{CuK}\alpha$ radiation. Average crystallite size D was calculated from the widths $\Delta 2\theta_{1/2}$ in the characteristic peaks with the Debye-Scherrer formula [24]. The Rietveld refinement of the XRD profile was carried out with the FullProf (Version 3.5d Oct98-LLB-JRC) program. The proposed structural model developed here is based on the coexistence of tetragonal (P4mm) [12, 25]

and hexagonal (R3c) phases [26, 27] for the $\text{PbZr}_{0.5}\text{Ti}_{0.5}\text{O}_3$ composition (Table 1). The external details of the particles and their morphology were studied with a transmission electron microscope (Model CM-12, Philips). The dielectric constant (ϵ) and Curie temperature (T_C) of the pellets with silver electrodes sintered at 1100 °C for 1 h were studied with an inductance-capacitance-resistance meter (HP-4192A). The specific surface area was measured by the single point BET method with liquid N_2 (Flowsorb 2300, Micromeritics Instrument Corp., Norcross, GA).

3. Results and discussion

Fig. 1 shows the X-ray diffractograms of $\text{PbZr}_{0.5}\text{Ti}_{0.5}\text{O}_3$ nanopowders processed by heating the polymeric precursor in air at (a) 400 °C (b) 500 °C (c) 600 °C and (d) 700 °C for 2 h. According to the diffraction pattern (Fig. 1a), $\text{PbZr}_{0.5}\text{Ti}_{0.5}\text{O}_3$ forms nanoparticles on heating the polymeric precursor at temperature as low as 400 °C for 2 h. Only a small impurity intermediate pyrochlore phase (10 to 15 %, according to the intensity in the prominent peaks) produced during the formation of PZT at intermediate temperatures [28, 29], is observed. Fig. 1a, thus, indicates a weak peak at an interplanar spacing 'd' of 0.3059 nm (marked by *) corresponding to the residual pyrochlore phase.

The intensity of this phase decreases prominently on heating the polymeric precursor at relatively higher temperatures and the peak at $d = 0.3059$ nm, no longer exists on heating the polymeric precursor at 700 °C for 2 h. Fig. 1d indicates the well-defined X-ray diffraction peaks of tetragonal $\text{PbZr}_{0.5}\text{Ti}_{0.5}\text{O}_3$, caused by heating the polymeric precursor at 700 °C for 2 h. The peaks observed in the diffractogram in Fig. 1d are assigned in Table 2 in terms of the Miller indices (hkl) assuming a tetragonal crystal structure of PZT [30] with lattice parameters $a = 0.4036$ nm and $c = 0.4147$ nm. This is a much simpler diffractogram (with a total of only eleven peaks over the almost entire 2θ region of 20 to 85°) in comparison to that of $\text{PbZr}_{0.5}\text{Ti}_{0.5}\text{O}_3$ in MPB phase, which has

a total of over twenty five peaks in this region with $a = 0.4036$ nm and $c = 0.4146$ nm [30].

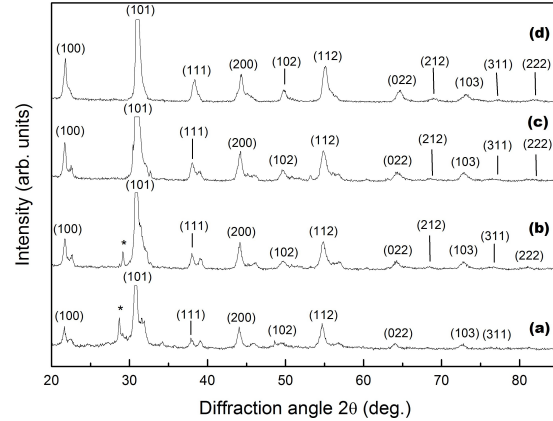


Fig. 1. X-ray diffractograms of $\text{PbZr}_{0.5}\text{Ti}_{0.5}\text{O}_3$ nanopowders processed by heating the polymeric precursor at (a) 400 °C (b) 500 °C (c) 600 °C and (d) 700 °C, for 2 h in air.

The most intense peak (relative intensity $I = 100$ %) in the diffractogram lies at 0.2892 nm in (101) reflection. The second and third most intense peaks lie in (100) and (112) reflections at 0.4034 nm ($I = 22$) and 0.1678 nm ($I = 19$), respectively. However, the diffractogram in Fig. 1(d) involves some satellite peaks, which are more distinct at 0.3965, 0.2007 and 0.1641 nm. This is possible because of the presence of hexagonal phase [26], which often coexists in the MPB composition [31]. A similar X-ray diffractogram have been reported by Sorowiak and coworkers for nanocrystalline tetragonal $\text{PbZr}_{0.5}\text{Ti}_{0.5}\text{O}_3$, obtained by conventional ceramic sintering at 927 °C [20].

Fig. 2 demonstrates Rietveld refinement for the X-ray diffractogram of $\text{PbZr}_{0.5}\text{Ti}_{0.5}\text{O}_3$ nanopowders processed by heating the polymeric precursor at 700 °C for 2 h in air (1d). It provides the precise information about the amount and the lattice parameters of the tetragonal phase in the as prepared $\text{PbZr}_{0.5}\text{Ti}_{0.5}\text{O}_3$ nanopowders. This infers the P4mm tetragonal crystal structure with $a = 0.4036$ nm and $c = 0.4147$ nm. In addition with tetragonal symmetry, a hexagonal symmetry (R3c) with $a = 0.5774$ nm and $c = 1.4212$ nm,

Table 1. The model used for the structural refinement of $\text{PbZr}_{0.5}\text{Ti}_{0.5}\text{O}_3$.

Tetragonal phase (P4mm)						Hexagonal phase (R3c)					
	x	y	z	occ	socc		x	y	z	occ	socc
Pb^{2+}	0	0	0	0.125	0	Pb^{2+}	0	0	0	0.333	0
Zr^{4+}	0.5	0.5	z	0.033	6	Zr^{4+}	0	0	z	0.227	8
Ti^{4+}	0.5	0.5	z	0.092	6	Ti^{4+}	0	0	z	0.106	8
O_1^{2-}	0.5	0.5	z	0.125	0	O_1^{2-}	0.172	0.344	z	1.0	0
O_2^{2-}	0.5	0	z	0.250	0	O_2^{2-}	0.655	0.828	z	1.0	0
a (nm)	0.4036					a (nm)	0.5788				
c (nm)	0.4146					c (nm)	1.430				

Table 2. Interplanar spacing (d_{hkl}) and relative intensities (I) in X-ray diffraction peaks in $\text{PbZr}_{0.5}\text{Ti}_{0.5}\text{O}_3$ nanopowders prepared through a polymeric precursor method.

d_{hkl} (nm)		I	h	k	l
Observed	Calculated				
0.4034	0.4037	22	1	0	0
0.2892	0.2891	100	1	0	1
0.2353	0.2352	13	1	1	1
0.2019	0.2021	15	2	0	0
0.1842	0.1844	06	1	0	2
0.1678	0.1679	19	1	1	2
0.1447	0.1445	07	0	2	2
0.1362	0.1361	03	2	1	2
0.1307	0.1306	04	1	0	3
0.1222	0.1221	<01	3	1	1
0.1175	0.1174	01	2	2	2

The sample has been calcined at 700 °C for 2 h. The calculated d_{hkl} values refer to average lattice parameters $a = 0.4036$ nm and $c = 0.4147$ nm in tetragonal structure [30].

has also been detected from the Rietveld refinement analysis.

The value of D for the $\text{PbZr}_{0.5}\text{Ti}_{0.5}\text{O}_3$ sample, processed at (a) 400 °C, (b) 500 °C, (c) 600 °C and (d) 700 °C for 2 h, vary from 20 nm in (a) to 21 nm in (b), 23 nm in (c) and 27 nm in (d). These D values refer to average values calculated by $\Delta 2\theta_{1/2}$ in the (101), (100), (111), (200) and (112) prominent peaks of the diffractograms. The D values

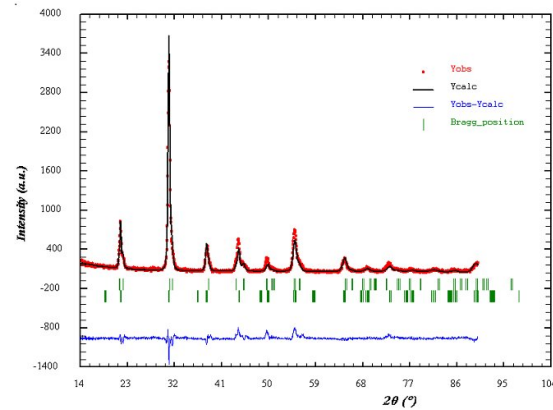


Fig. 2. Rietveld refinement for the X-ray diffractogram of $\text{PbZr}_{0.5}\text{Ti}_{0.5}\text{O}_3$ nanopowders processed by heating the polymeric precursor at 700 °C for 2 h in air.

were also calculated applying Williamson-Hall integral breadth method [32]. In this method the selected peaks were fitted in a computer program. With this program the value of $\sin\theta$ and β (FWHM) were calculated for each peak. D values were obtained from the intercept of the plot of β vs. $\sin\theta$ of the prominent peaks, using the relation:

$$\beta = 1/D + 4e \cdot \sin \theta / \lambda \quad (1)$$

where β – FWHM; D – crystallite size, e – microstrain in the sample, 2θ – diffraction angle, λ – wavelength [33]. The calculated D values by both the methods are nearly same.

The average particle size, D has also been estimated with the help of the specific surface area,

measured by BET method with the relation:

$$D_{BET} = 6/(\langle \rho \rangle \cdot S_{BET}) = 26.101 \text{ nm} \quad (2)$$

where $\langle \rho \rangle$ is density and S_{BET} is the specific surface area ($34 \text{ m}^2/\text{g}$) of the as prepared $\text{PbZr}_{0.5}\text{Ti}_{0.5}\text{O}_3$ powders.

Fig. 3 shows (a) the bright field TEM micrograph and (b) the corresponding SAED pattern of $\text{PbZr}_{0.5}\text{Ti}_{0.5}\text{O}_3$ nanopowders processed at 700°C for 2 h. Fig. 3a shows small granules of $\text{PbZr}_{0.5}\text{Ti}_{0.5}\text{O}_3$ nanopowders of nearly spherical shapes. The size of the granules in Fig. 3a varies from 25 to 27 nm. A close comparison of their sizes with the D values suggests that they are single crystallites. The SAED pattern in Fig. 3b, which has been taken from the region of 3a, consists of two concentric rings at 0.2889 and 0.2018 nm with the arrays of spots in the (100), (101) and (200) lattice reflections. This is a typical pattern of a nanocrystalline solid. The two d_{hkl} values reasonably match with those of the (101) and (200) reflections in the X-ray diffraction pattern at 0.2892 and 0.2022 nm, respectively (Table 1). In the two reflections roughly the same intensity ratio was found as in the X-ray diffraction patterns.

The as prepared $\text{PbZr}_{0.5}\text{Ti}_{0.5}\text{O}_3$ nanopowder exhibits ferroelectric properties. As in normal ferroelectrics, the ϵ value increases gradually, as a function of temperature, and reaches a maximum ϵ_{max} value at $T_C \sim 370^\circ\text{C}$ at 1 kHz (Fig. 4). The value of ϵ_{max} is found to be 25000 with $\epsilon = 1100$ at room temperature at 1 kHz. The present values are comparable with the values obtained in similar PZT nanoceramics prepared by sol gel and other methods [28, 29]. The reduction of T_C in $\text{PbZr}_{0.5}\text{Ti}_{0.5}\text{O}_3$ nanopowder, in the present investigation, in comparison to the well established reported value [1] in $\text{PbZr}_{0.52}\text{Ti}_{0.48}\text{O}_3$ ceramic powder, is presumed to be due to the effect of depolarization field [34].

The high value of ϵ in $\text{PbZr}_{0.5}\text{Ti}_{0.5}\text{O}_3$ nanopowder, in the present investigation, is probably caused by strong surface dipolar interactions in $\text{PbZr}_{0.5}\text{Ti}_{0.5}\text{O}_3$ nanoparticles, as demonstrated in Fig. 5. The surface dipolar interactions may be the major contributor to the high surface energy of $\text{PbZr}_{0.5}\text{Ti}_{0.5}\text{O}_3$ nanoparticles; one should also

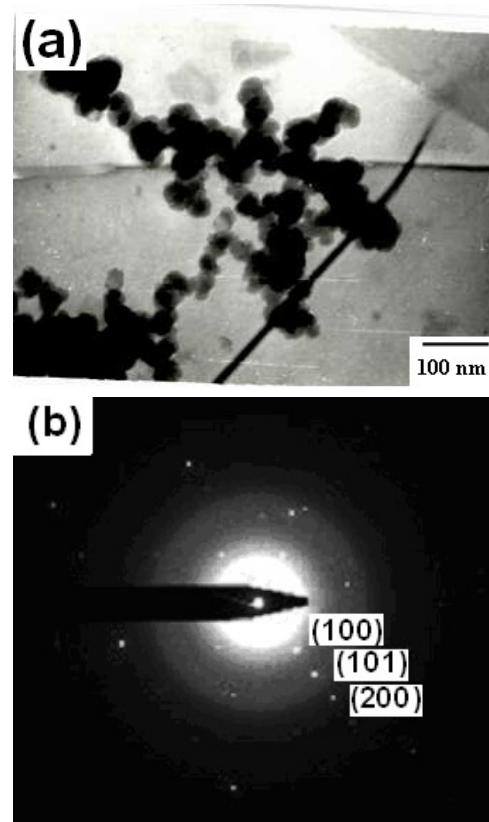


Fig. 3. (a) Bright field TEM micrograph and (b) SAED, of $\text{PbZr}_{0.5}\text{Ti}_{0.5}\text{O}_3$ nanopowders processed by heating the polymeric precursor at 700°C for 2 h in air.

consider other effects, such as surface reconstruction and next neighbour interactions, etc. [35].

4. Conclusions

Polymeric precursor method has been exploited for the preparation of $\text{PbZr}_{0.5}\text{Ti}_{0.5}\text{O}_3$ nanoparticles with a P4mm tetragonal crystal structure, by heating the precursor material at 700°C for 2 h. The advantage of this method is that as prepared polymer precursor decomposes with combustion at temperatures as low as 400°C , resulting in crystallized $\text{PbZr}_{0.5}\text{Ti}_{0.5}\text{O}_3$ nanopowders. The average crystallite size, calculated from $\Delta 2\theta_{1/2}$ in the XRD peaks using the Debye Scherrer relation varies from 20 to 25 nm. The average particle size (D) of $\text{PbZr}_{0.5}\text{Ti}_{0.5}\text{O}_3$ powders, estimated with the help of the specific surface

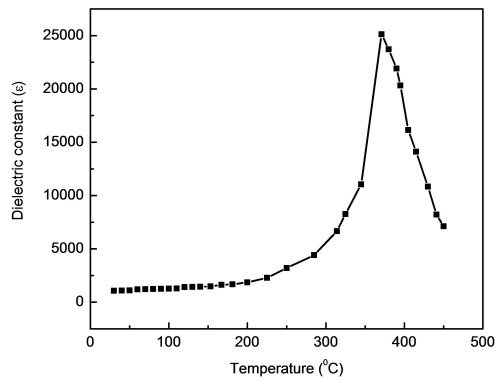


Fig. 4. Variation of dielectric constant of the as prepared $\text{PbZr}_{0.5}\text{Ti}_{0.5}\text{O}_3$ nanopowders with temperature.

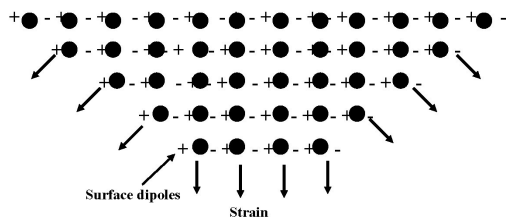


Fig. 5. Schematic view of a surface of a nanoparticle demonstrating the nature of the surface stresses due to inter-dipolar repulsion at the surface.

area, measured by BET method, is 26.1 nm. TEM study made it possible to measure the particle size of the $\text{PbZr}_{0.5}\text{Ti}_{0.5}\text{O}_3$ powders with an average diameter of 27 nm. The ϵ value in $\text{PbZr}_{0.5}\text{Ti}_{0.5}\text{O}_3$ nanopowders obtained in the present study indicates the applicability of the employed method for producing high quality $\text{PbZr}_{0.5}\text{Ti}_{0.5}\text{O}_3$ nanoceramics at moderate temperatures. Thus, the prepared nanocrystalline $\text{PbZr}_{0.5}\text{Ti}_{0.5}\text{O}_3$ materials have a wide scope for the utilization in super performance mini devices with small physical volume.

References

- [1] JAFFE B., COOK W.R., JAFFE H., *Piezoelectric Ceramics*, Academic Press, London, 1971, pp. 123 – 238.
- [2] UCHINO K., *Acta Mater.*, 46 (1998), 3745.
- [3] FUNAKUBO H., ARATANI M., OIKAWA T., TOKITA K., SAITO K., *J. Appl. Phys.*, 92 (2002), 6768.
- [4] ROELOFS A., SCHNELLER T., SZOT K., WASER R., *Nanotechnology*, 14 (2003), 250.
- [5] MANDAL T.K., RAM S., *Mater. Lett.*, 57 (2003), 2432.
- [6] MANDAL T.K., *Appl. Phys. Lett.*, 89 (2006), 034103.
- [7] SACHDEVA A., ARORA M., TANDON R.P., *J. Nanosci. Nanotechnol.*, 9 (2009), 6631.
- [8] MORITA T., *Materials*, 3 (2010), 5236.
- [9] CHAMOLA A., SINGH H., NAITHANI U.C., SHARMA S., PRABHAT U., DEVI PRATIKSHA., MALIK A., SRIVASTAVA A., SHARMA R.K., *Adv. Mater. Lett.* 2 (2011), 26.
- [10] MISRI I., HAREESH P., YANG S Y., DEVOE D.L., *J. Micromech. Microeng.*, 22 (2012), 085017.
- [11] MANDAL T.K., *Indian J. Phys.*, 86 (2012), 818.
- [12] SRIVASTAVAN G., GOSWAMI A., UMARJI A.M., *Ceram. Int.*, 39 (2013), 1977.
- [13] RAGINI, MISHRA S.K., PANDEY D., *Phys. Rev. B.*, 64 (2001), 054101.
- [14] NOHEDA B., GONJALO J.A., CROSS L.E., GUO R., PARK S.E., COX D.E., SHIRANE G., *Phys. Rev. B.*, 61 (2000), 8687.
- [15] KLEE M., VEIMAN A.D., WASER R., BRAND W., HAL H.V., *J. Appl. Phys.*, 72 (1992), 1566.
- [16] GOLDBERG R.L., SMITH S.W., *IEEE T. Ultrason. Ferr.*, 41 (1994), 761.
- [17] KONG L.B., MA J., ZHANG R.F., ZHU W., TAN O.K., *Mater. Lett.*, 55 (2002), 370.
- [18] HAMMER M., HOFFMANN M.J., BARETZKY B.J., *J. Eur. Ceram. Soc.*, 1 (1996), 161.
- [19] SAHA S.K., AGARWAL D.C., *Am. Ceram. Soc. Bull.*, 71 (1992), 1424.
- [20] SOROWIAK Z., KUPRIYANOV M.F., CZEKAJ D.J., *J. Eur. Ceram. Soc.*, 21 (2001), 1377.
- [21] ZENG J., SONG S., WANG L., ZHANG M. Z., ZHENG L., LIN C., *J. Am. Ceram. Soc.*, 82 (1999), 461.
- [22] WU A., VILARINHO P.M., SALVADO I.M.M., BAPTISTA J.L., *J. Am. Ceram. Soc.*, 83 (2000), 1379.
- [23] MALIC B., KOSEC M., *J. Sol-gel Sci. Techn.*, 2 (1994), 443.
- [24] KLUG M.P., L.E. ALEXANDER, *X-ray Diffraction Procedure for Polycrystalline and Amorphous Materials*, Wiley, New York, 1974. p. 634.
- [25] RAGINI, RANJAN R., MISHRA S.K., PANDEY D., *J. Appl. Phys.*, 92 (2002), 3266.
- [26] JCPDS X-ray powder diffraction file, 861710, *Hexagonal $\text{PbZr}_{0.75}\text{Ti}_{0.25}\text{O}_3$* .
- [27] MEGAW H.D., DARLINGTON C.N.W., *Acta. Crystallogr. A*, 31 (1975), 161.
- [28] PARK H.B., PARK C.Y., HONG Y.S., KIM K., KIM S.J., *J. Am. Ceram. Soc.*, 82 (1999), 94.
- [29] SHAO Q., LI A., LING H., WU D., WANG Y., MING N., *Mater. Lett.*, 50 (2001), 32.
- [30] JCPDS X-ray powder diffraction file, 33-0784, *Tetragonal $\text{PbZr}_{0.52}\text{Ti}_{0.48}\text{O}_3$* .
- [31] NASAR R.S., CERQUEIRA M.C., LONGO E.L., LEITE E.R., VARELA J.A., ANDRES B.J., *J. Mater. Sci.*, 34 (1999), 3659.
- [32] LUCKS I., LAMPARTER P., MITTEMEIJER E.J., *J. Appl. Cryst.*, 37 (2004), 300.

- [33] MANDAL T.K., *Mater. Lett.*, 61 (2007), 850.
- [34] BEGG B.D., VANCE E.R., NOWOTNY J., *J. Am. Ceram. Soc.*, 77 (1994), 3186.
- [35] AYYUB P., *Phys. Edun.*, 1 (1998) 309.

Received 2013-09-10

Accepted 2015-01-16